TISSUE ENGINEERING: Part A
Volume 20, Numbers 17 and 18, 2014

DOI: 10.1089/ten.tea.2013.0400

Collagen-GAG Scaffold Biophysical Properties Bias MSC Lineage Choice in the Presence of Mixed Soluble Signals

Steven R. Caliari, PhD,[1] and Brendan A.C. Harley, ScD[1,2]

Biomaterial strategies for regenerating multitissue structures require unique approaches. One strategy is to design scaffolds so that their local biophysical properties can enhance site-specific effects of an otherwise heterogeneous biomolecular environment. This investigation examined the role of biomaterial physical properties (relative density, mineral content) on the human mesenchymal stem cell phenotype in the presence of mixed soluble signals to drive osteogenesis or chondrogenesis. We tested a series of three-dimensional collagen–glycosaminoglycan scaffolds with properties inspired by extracellular matrix characteristics across the osteotendinous interface (tendon, cartilage, and bone). We found that selective scaffold mineralization induced a depressed chondrogenic response compared with nonmineralized groups as demonstrated by gene expression and histological analyses. Interestingly, the greatest chondrogenic response was found in a higher density, nonmineralized scaffold variant despite increased contraction and cellular condensation in lower density nonmineralized scaffolds. In fact, the lower density scaffolds demonstrated a significantly higher expression of osteogenic transcripts as well as ample mineralization after 21 days of culture. This effect may be due to local stiffening of the scaffold microenvironment as the scaffold contracts, leading to increased cell density, accelerated differentiation, and possible endochondral ossification as evidenced by a transition from a glycosaminoglycan (GAG)-rich milieu to higher mineralization at later culture times. These findings will help shape the design rules for graded biomaterials to regenerate distinct fibrillar, fibrocartilagenous, and mineralized regions of orthopedic interfaces.

Introduction

Orthopedic interfaces such as osteochondral and osteotendinous junctions contain gradations of extracellular matrix (ECM) components, both organic (e.g., collagens, proteoglycans) and inorganic (e.g., hydroxyapatite mineral).[1–3] Additionally, a mixed set of soluble regulators of cell behavior, such as growth factors and cytokines, reside within these graded interfaces.[4] Tissue engineering strategies, for spatially graded, multitissue structures, therefore require a nuanced understanding of both soluble and insoluble (microstructural, mechanical, and compositional) regulators of cell behavior.

An emerging paradigm for scaffold design in orthopedic interface engineering is the creation of biomaterials containing spatially ordered biophysical and/or biochemical properties. Such multicompartment biomaterials may be used to drive spatially defined mesenchymal stem cell (MSC) differentiation or alternatively support the activity of multiple compartment-specific differentiated cell types (e.g., fibroblasts, chondrocytes, and osteoblasts).[5–7] Whereas directing MSC differentiation in a spatially selective manner may become a more efficient and clinically viable approach, it is difficult to selectively regulate differentiation through material properties alone.

The most common approach for driving MSC differentiation *in vitro* is the application of lineage-specific media cocktails containing various soluble factors (e.g., small molecules, amino acids, cytokines, and/or steroids). Although these differentiation media have been used extensively to drive osteogenic, chondrogenic, and adipogenic MSC differentiation,[8] their usefulness is limited when trying to recapitulate the dynamic microenvironments of multitissue structures, where graded, and sometimes, competing, soluble and insoluble signals influence the phenotype of multiple classes of differentiated cell types.

As a first order solution, mixed media formulations using combinations of osteogenic, chondrogenic, and/or adipogenic media may be applied to cell–biomaterial constructs. In this study, biomaterial characteristics may bias cell responses to a cocktail of signals containing multiple, disparate differentiation cues. To better design such systems, it is important to unravel the role material properties play on MSC differentiation potential in the presence of multiple competing soluble cues. This approach has been extensively applied in combined osteogenic–adipogenic[9,10] and

[1]Department of Chemical and Biomolecular Engineering, University of Illinois at Urbana-Champaign, Urbana, Illinois.
[2]Institute for Genomic Biology, University of Illinois at Urbana-Champaign, Urbana, Illinois.

osteogenic–chondrogenic environments.[11] These studies revealed the influence of properties such as the elastic modulus, pore size, ligand density, and chemical composition on MSC-lineage specification and signal transduction. Critically, these studies represent a paradigm shift away from designing biomaterials that simply enhance the effects of soluble factors. Instead, they suggest that through improved understanding of the role material properties play in differentiation potential, the stem cell fate can be biased toward specific lineages in the presence of heterogeneous biomolecular environments more analogous to those encountered *in vivo*.

This study explores the potential for systematic alteration of a collagen–glycosaminoglycan (CG) scaffold platform to bias osteogenic versus chondrogenic MSC differentiation. CG biomaterials have been used in diverse regenerative medicine applications ranging from clinical treatment of skin[12] and peripheral nerve[13] defects to use as model systems to address fundamental questions about cellular processes such as adhesion,[14] motility,[15] and differentiation.[16] This article describes the influence of CG scaffold relative density and mineral content on the differentiation potential of MSCs in the presence of mixed osteogenic and chondrogenic signals. We investigated three scaffold groups: a low-density nonmineralized scaffold that we hypothesized to be amenable to chondrogenesis,[16,17] a higher density variant with superior mechanical competence more suitable for tendon/ligament tissue engineering,[18] and a mineralized CG scaffold previously developed for bone tissue engineering applications.[19] Whereas variants of these scaffolds have previously been shown to support separate osteogenic and chondrogenic MSC differentiation in the presence of differentiation media,[16] the impact of CG scaffold physical properties, such as relative density and mineral content, on biasing MSC differentiation in the presence of competing soluble signals has not been evaluated. Further, elucidating the influence of scaffold physical properties on MSC-lineage specification would inform the design of materials to regenerate multitissue structures such as osteochondral and osteotendinous interfaces.

Materials and Methods

All reagents were purchased from Sigma-Aldrich (St. Louis, MO) unless otherwise specified.

Precursor suspension preparation

Three different collagen-glycosaminoglycan (GAG) suspensions were prepared to make low-density, high-density, and mineralized CG scaffold variants. Low-density and high-density nonmineralized CG suspensions consisted of type I collagen from the bovine Achilles tendon and chondroitin sulfate in 0.05 M acetic acid.[20] Suspensions were prepared at 0.5% or 1.5% w/v collagen (collagen:GAG ratio of 11.25:1) for the low- versus high-density variants, respectively. Calcium phosphate-mineralized collagen-GAG (CGCaP) suspension was produced from collagen (1.9 w/v%) and GAG (0.84 w/v%) as before, along with calcium salts ($Ca(OH)_2$, $Ca(NO_3)_2 \cdot 4H_2O$) in phosphoric acid. A titrant-free concurrent mapping method was used to generate the CGCaP suspension that yielded scaffolds with 40 wt% mineral content.[21]

Scaffold fabrication through freeze-drying

Scaffolds were fabricated through lyophilization in a Genesis freeze-dryer (VirTis, Gardiner, NY) using a constant cooling rate method as previously described.[22] Briefly, CG or CGCaP suspensions were degassed and added to $3'' \times 3''$ polysulfone freeze-drying molds, then cooled at a constant rate of 1°C/min to a final freezing temperature of -10°C. The suspensions were maintained at this temperature for 2 h to completely freeze the suspension followed by sublimation of the ice crystals at 0°C and 200 mTorr to produce dry scaffolds with pores $>150\,\mu$m.[18,23]

Scaffold crosslinking and hydration

CG scaffolds were dehydrothermally crosslinked at 105°C for 24 h under vacuum (<25 torr) in a vacuum oven (Welch, Niles, IL) following lyophilization. Scaffolds were sterilized in ethanol and rinsed several times in phosphate-buffered saline (PBS) before use. Additional chemical crosslinking for all CG and CGCaP scaffolds was performed using a mixture of 1-ethyl-3-[3-dimethylaminopropyl] carbodiimide hydrochloride (EDC) and *N*-hydroxysulfosuccinimide (NHS) at a molar ratio of 5:2:1 EDC:NHS:COOH, where COOH represents the scaffold carboxyl (collagen) content,[24,25] in PBS for 1.5 h at 25°C.

Cell culture

Human bone marrow-derived MSCs were purchased from Lonza (Walkersville, MD). The MSCs were cultured in a complete MSC growth medium purchased from the manufacturer (Lonza) at 37°C and 5% CO_2, fed twice a week, and used at passage 6 for all experiments.

Cell-seeded scaffold culture conditions

CG and CGCaP scaffold pieces (6 mm diameter, 3 mm thickness) were seeded with MSCs using a previously validated static seeding method.[14] Briefly, scaffolds were partially dried with Kimwipes and seeded with 7.5×10^4 MSCs per 20 μL media (10 μL on each side of scaffold) in ultralow attachment six-well plates (Corning Life Sciences, Lowell, MA). Cells were allowed to attach for 2.5 h before adding media to well plates. Cell-seeded scaffolds were cultured at 37°C and 5% CO_2 and fed twice a week with a 1:1 mix of osteogenic and chondrogenic differentiation media as supplied by Lonza. For histology studies, control scaffolds were cultured in standard growth media (Lonza).

MSC metabolic activity quantification

The mitochondrial metabolic activity of MSCs seeded within scaffold pieces was quantified using the alamarBlue® assay.[26] Cell-seeded scaffolds were incubated in the alamarBlue solution (Invitrogen, Carlsbad, CA) with gentle shaking for 2 h. The reduction of resazurin in the solution by metabolically active cells to the fluorescent by-product resorufin was measured on a fluorescent spectrophotometer (Tecan, Männedorf, Switzerland).

Quantification of scaffold contraction

The diameter of each scaffold piece was measured at the 1-, 7-, 14-, and 21-day time points using standard drafting

templates and normalized against a starting scaffold diameter at day 0 to determine scaffold contraction as previously described.[27] Cellular solids modeling was used to predict changes in the scaffold elastic modulus (E^*) as a function of scaffold contracted diameter (d) where E^* is proportional to d^{-6}.[28]

RNA isolation, reverse transcription, and real-time polymerase chain reaction

Isolation of RNA from MSC-seeded scaffolds was performed at day 7, 14, and 21 time points using an RNeasy Plant Mini kit (Qiagen, Valencia, CA).[18,29] Scaffolds were rinsed with PBS and then added to the RLT lysis buffer (supplied with the kit) supplemented with β-mercaptoethanol for 5 min on ice. Scaffolds were disrupted with QIAshredder columns and the lysates were processed following the kit instructions to isolate RNA. RNA was then reverse transcribed to cDNA in a Bio-Rad S1000 thermal cycler using the QuantiTect Reverse Transcription kit (Qiagen). Real-time polymerase chain reactions (PCR) were performed in triplicate using the QuantiTect SYBR Green PCR (Qiagen) kit in an Applied Biosystems 7900HT Fast Real-Time PCR System (Applied Biosystems, Carlsbad, CA). All primer sequences used were taken from the literature[30,31] (Table 1) and were synthesized by Integrated DNA Technologies (Coralville, IA). Expression levels of the chondrogenic markers collagen type II alpha 1 (*COL2A1*), aggrecan (*ACAN*), and sex determining region Y box 9 (*SOX9*) as well as osteogenic markers runt-related transcription factor 2 (*RUNX2*), bone sialoprotein (*BSP*), alkaline phosphatase (*ALP*), and osteocalcin (*OCN*) were quantified with glyceraldehyde 3-phosphate dehydrogenase (*GAPDH*) used as a housekeeping gene. Data were analyzed using Sequence Detection Systems software v2.4 (Applied Biosystems) using the delta-delta Ct method and all results were expressed as fold changes normalized to the expression levels of MSCs cultured in the high-density CG scaffolds at day 7.

Histology

Cell-seeded scaffolds at days 7, 14, and 21 were fixed in 10% neutral buffered formalin for histological analyses. Fixed scaffold pieces were embedded in paraffin and sequentially sliced into 5-μm-thick sections. Sections were deparaffinized and stained with hematoxylin and eosin (H&E) to visualize cellular organization within scaffolds, Alizarin red to assess mineral content, and Alcian blue to determine GAG content.

Statistical analysis

Two-way analysis of variance was performed on the metabolic activity, scaffold diameter, and gene expression data sets (independent variable time and scaffold type) followed by Tukey-honest significant difference *post hoc* tests. Significance was set at $p < 0.05$. Scaffolds from three independent experiments were analyzed at each time point for all metrics. Error is reported in figures as the standard error of the mean unless otherwise noted.

Results

Scaffold contraction and metabolic activity

Previous efforts have shown that hydrated, crosslinked acellular CG scaffolds can maintain network integrity for multiple weeks.[16,32,33] However, cell-mediated contraction of CG scaffolds is commonly observed,[18,34] so we measured scaffold contraction after days 1, 7, 14, and 21 of culture (Fig. 1A). High-density nonmineralized scaffolds showed minor contraction, while mineralized scaffolds did not contract over the entire course of the experiment. However, low-density nonmineralized scaffolds showed an early loss of structural integrity that was maintained throughout the experiment.

All experimental groups demonstrated sustained metabolic activity over the course of the 21-day experiment (Fig. 1B). The metabolic activity was initially significantly higher in the high-density nonmineralized group at day 7 ($p < 0.03$). On

Table 1. Primer Sequences from Literature Used for Polymerase Chain Reaction

Transcript	*Sequence*	*Reference*
ACAN	Forward: 5′-TGCATTCCACGAAGCTAACCTT-3′ Reverse: 5′-GACGCCTCGCCTTCTTGAA-3′	31
ALP	Forward: 5′-AGCACTCCCACTTCATCTGGAA-3′ Reverse: 5′-GAGACCCAATAGGTAGTCCACATTG-3′	31
BSP	Forward: 5′-TGCCTTGAGCCTGCTTCC-3′ Reverse: 5′-GCAAAATTAAAGCAGTCTTCATTTTG-3′	30
COL2A1	Forward: 5′-GGCAATAGCAGGTTCACGTACA-3′ Reverse: 5′-CGATAACAGTCTTGCCCCACTT-3′	31
GAPDH	Forward: 5′-AGAAAAACCTGCCAAATATGATGAC-3′ Reverse: 5′-TGGGTGTCGCTGTTGAAGTC-3′	31
OCN	Forward: 5′-CAGCGAGGTAGTGAAGAGA-3′ Reverse: 5′-GAAAGCCGATGTGGTCAG-3′	31
RUNX2	Forward: 5′-AGAAGGCACAGACAGAAGCTTGA-3′ Reverse: 5′-AGGAATGCGCCCTAAATCACT-3′	31
SOX9	Forward: 5′-AGCGAACGCACATCAAGAC-3′ Reverse: 5′-GCTGTAGTGTGGGAGGTTGAA-3′	31

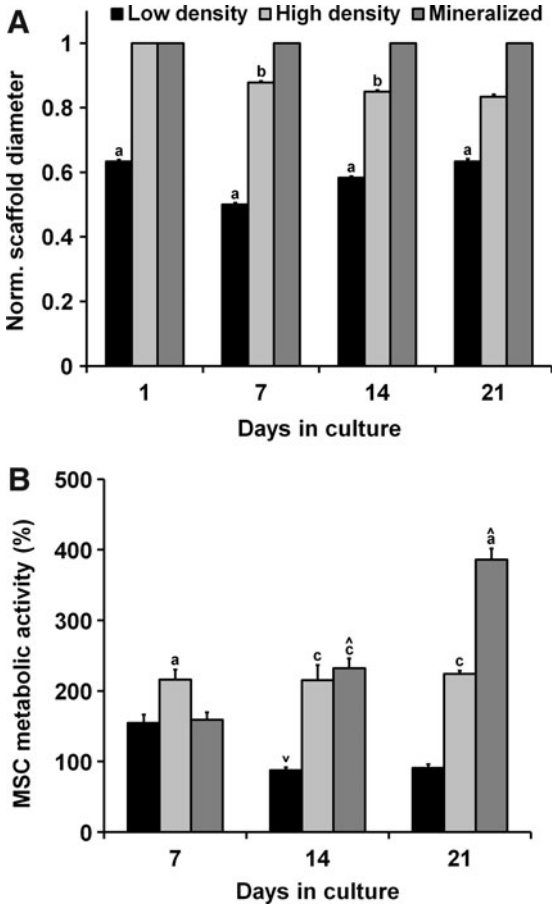

FIG. 1. MSC contraction and metabolic activity as a function of time and scaffold type. **(A)** Pronounced cell-mediated contraction was observed for the low-density group with minor contractions in the high-density group and negligible contraction in the mineralized scaffold group. **(B)** Human MSCs remained metabolically active over extended culture times. [a]Significantly different from other two experimental groups, [b]significantly different from the mineralized group, [c]significantly different from the low-density group, ^significantly increased from previous time point, and ˇsignificantly decreased from previous time point. MSC, mesenchymal stem cell.

day 14, the activity significantly decreased in the low-density group ($p = 0.01$), held steady in the high-density group, and significantly increased in the mineralized group ($p = 0.009$), with the low-density group having a significantly lower metabolic activity than the other two experimental groups ($p < 0.0009$). The metabolic activity for the low- and high-density nonmineralized groups remained relatively constant from day 14 to 21, while the mineralized group showed a significant increase ($p = 0.0003$). The mineralized and high-density nonmineralized scaffold groups maintained a significantly higher metabolic activity than the lower density nonmineralized group ($p < 0.0003$) at the completion of the experiment.

Trends in chondrogenic gene expression

The expression of chondrogenic genes *COL2A1*, *ACAN*, and *SOX9* was measured after 7, 14, and 21 days in culture (Fig. 2). Statistical analyses revealed a significant influence of both culture time and scaffold type on the expression of *COL2A1* and *ACAN* ($p < 0.05$). Elevated levels of *COL2A1* were observed in the nonmineralized scaffold groups with significantly higher expressions in the

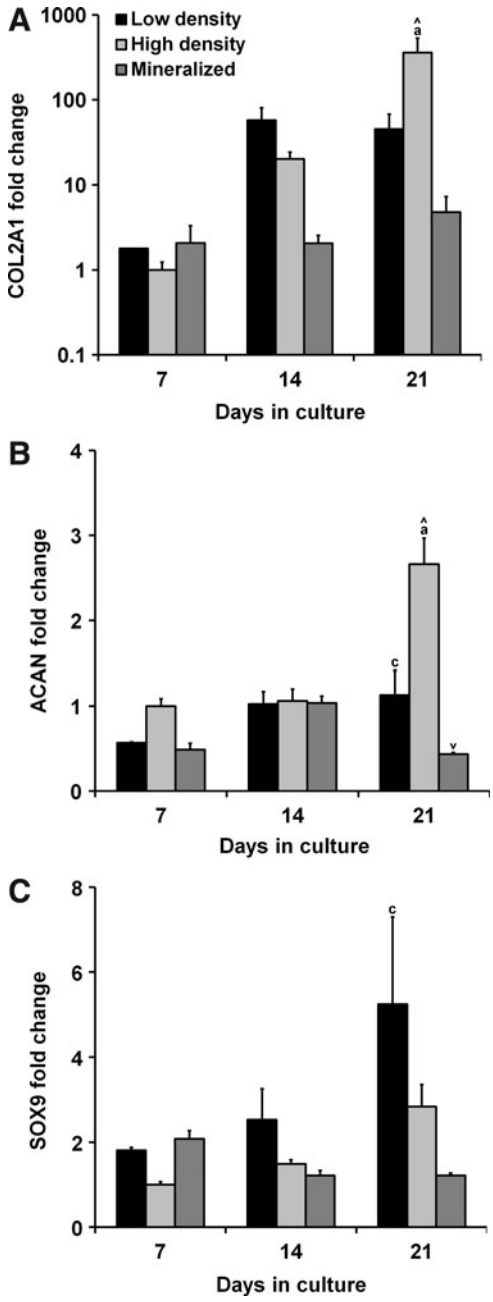

FIG. 2. Trends in chondrogenic gene expression. Expression profiles of chondrogenic genes **(A)** collagen type II alpha 1 (*COL2A1*), **(B)** aggrecan (*ACAN*), and **(C)** sex determining region Y box 9 (*SOX9*) were tracked for 21 days. After 21 days, expression levels of all three transcripts were depressed in the mineralized group with significantly higher expression of *COL2A1* and *ACAN* observed in the high-density group. [a]Significantly different from other two experimental groups, [c]significantly different from the mineralized group, ^significantly increased from previous time point, and ˇsignificantly decreased from previous time point.

higher density nonmineralized group compared with the other groups at day 21 ($p < 0.02$) (Fig. 2A). These results were largely mirrored in the *ACAN* expression profile with significantly higher expressions at day 21 in the high-density nonmineralized group ($p < 0.002$) as well as significantly higher expressions at day 21 in the lower density group compared with the mineralized scaffolds ($p = 0.03$) (Fig. 2B). *SOX9* expression was also elevated in the nonmineralized groups compared with the mineralized group at day 21 with significantly higher expressions in the low-density nonmineralized group compared with the mineralized group ($p = 0.01$) (Fig. 2C).

Trends in osteogenic gene expression

The expression of osteogenic genes *RUNX2*, *BSP*, *ALP*, and *OCN* was measured after 7, 14, and 21 days in culture (Fig. 3). Statistical analyses revealed a significant influence of both culture time and scaffold type on expression of *BSP*, *ALP*, and *OCN* ($p < 0.008$). *RUNX2* expression in the mineralized scaffolds showed nonsignificant increases over the nonmineralized groups at days 7 and 14, peaking at day 14 before decreasing in day 21 (Fig. 3A). Meanwhile, the nonmineralized groups showed steady increases in *RUNX2* expression with significant increases between days 7 and 14 for the low-density group ($p = 0.04$) and between days 14 and 21 for the high-density group ($p = 0.005$). No significant differences were found between the groups for *BSP* expression at days 7 and 14 (Fig. 3B). However, *BSP* expression in the low-density nonmineralized group was significantly upregulated from day 14 to 21 and was significantly higher than the other groups at the day 21 time point ($p < 0.005$). There were no differences in *ALP* expression between the groups at day 7, but there was a significantly upregulated expression in the low-density nonmineralized group at each successive time point with a significantly higher overall expression than the other experimental groups at days 14 ($p < 0.03$) and 21 ($p < 0.0002$) (Fig. 3C). No significant differences in *OCN* expression between the groups were observed at days 7 and 14, but at day 21 there was a significant upregulation in the low-density nonmineralized group expression, resulting in significantly higher expression levels than the other two experimental groups ($p < 0.02$) (Fig. 3D).

Histology: H&E, Alizarin red, Alcian blue

Histological staining for cellular distribution, mineralization, and GAG content was undertaken using H&E, Alizarin red, and Alcian blue stains, respectively. We first assessed the MSC/scaffold organization through H&E staining (Fig. 4). Although MSC infiltration appeared similar in all experimental groups, staining clearly shows evidence of increased pore contraction and cellular condensation in the nonmineralized mixed media groups (Fig. 4B, D) compared with the corresponding growth media samples (Fig. 4A, C). Whereas the nonmineralized scaffold variants displayed little to no mineralization when cultured in growth media after 21 days (Fig. 5A, C), their counterparts cultured in mixed induction media showed significant mineralization by day 21 (Fig. 5B, D). There did not appear to be significant differences in mineralization between the mineralized (growth) (Fig. 5E) and mineralized (mixed) (Fig. 5F) media groups. Finally, we evaluated GAG distribution as a proxy for chondrogenesis using Alcian blue staining (Fig. 6). The biggest difference between the growth and mixed media pairs after 21 days

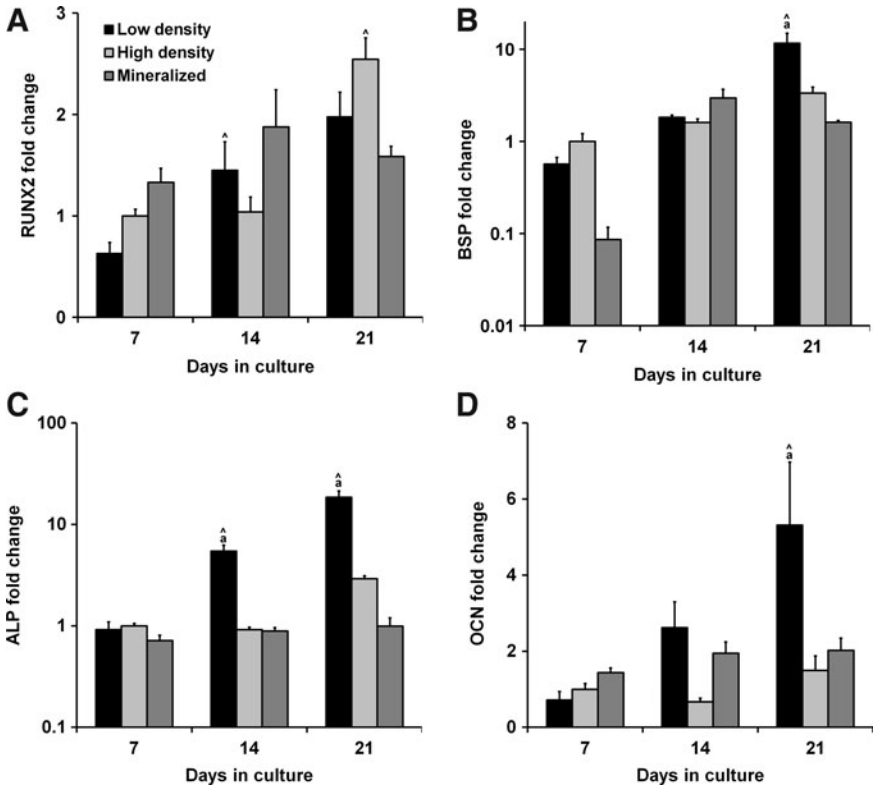

FIG. 3. Trends in osteogenic gene expression. Expression profiles of osteogenic genes **(A)** runt-related transcription factor 2 (*RUNX2*), **(B)** bone sialoprotein (*BSP*), **(C)** alkaline phosphatase (*ALP*), and **(D)** osteocalcin (*OCN*) were tracked for 21 days. After 21 days, *BSP*, *ALP*, and *OCN* were all significantly upregulated in the low-density nonmineralized group. [a]Significantly different from other two experimental groups and ^significantly increased from previous time point.

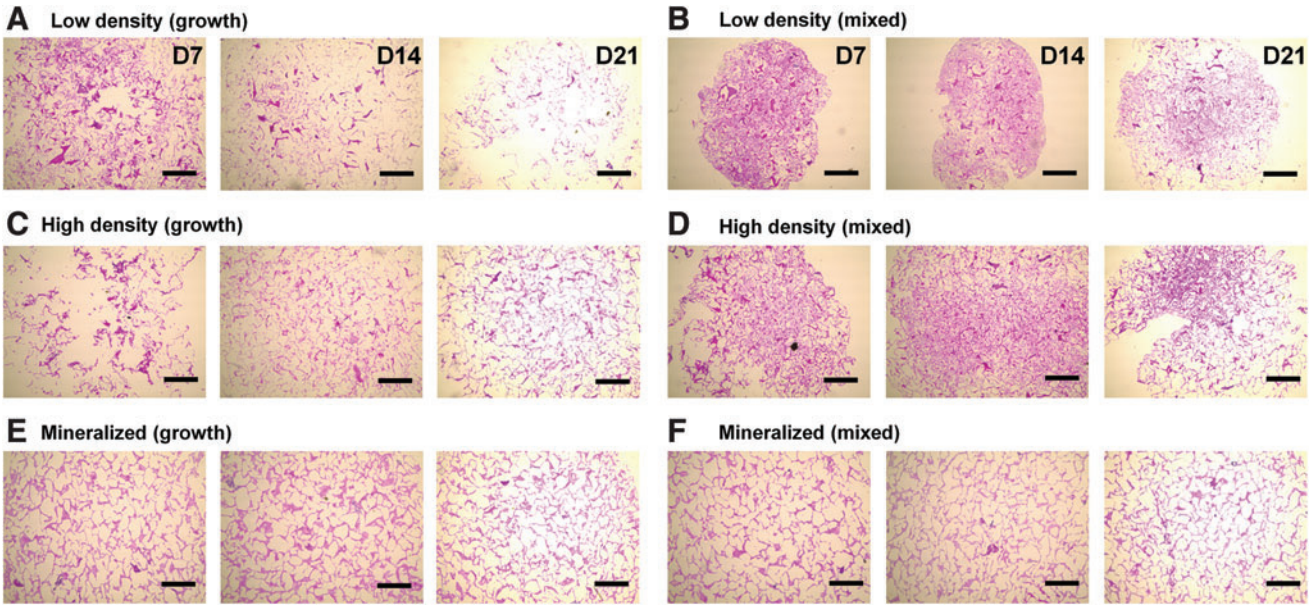

FIG. 4. Hematoxylin and eosin staining of scaffold sections. Histology sections show differences in MSC distribution and scaffold contraction. **(A)** Low density (growth), **(B)** low density (mixed), **(C)** high density (growth), **(D)** high density (mixed), **(E)** mineralized (growth), and **(F)** mineralized (mixed). Scale bars: 500 μm. Color images available online at www.liebertpub.com/tea

appears to be in the high-density, nonmineralized variant, where mixed media supported increased GAG staining (Fig. 6D). There appeared to be more GAG in the low-density mixed media groups compared with their growth media counterparts at days 7 and 14, although this difference was eliminated by day 21 (Fig. 6B).

Discussion

This study examined the effects of scaffold relative density and mineral content on MSC viability, phenotype, and ECM distribution over the course of three weeks in the presence of competing osteogenic and chondrogenic media

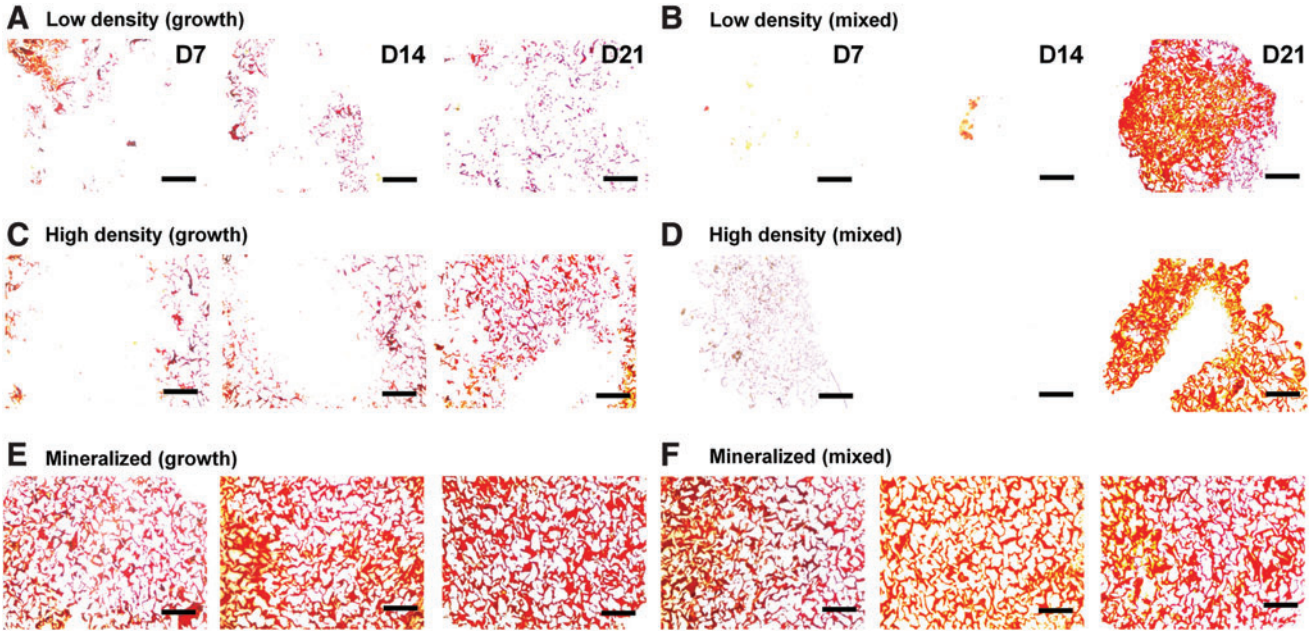

FIG. 5. Alizarin red staining of scaffold sections. Histology sections reveal differential mineral content as a function of scaffold type and media treatment with the nonmineralized scaffold groups showing little mineralization at days 7 or 14, but robust mineralization in the mixed media groups at day 21. **(A)** Low density (growth), **(B)** low density (mixed), **(C)** high density (growth), **(D)** high density (mixed), **(E)** mineralized (growth), **(F)** mineralized (mixed). Scale bars: 500 μm. Color images available online at www.liebertpub.com/tea

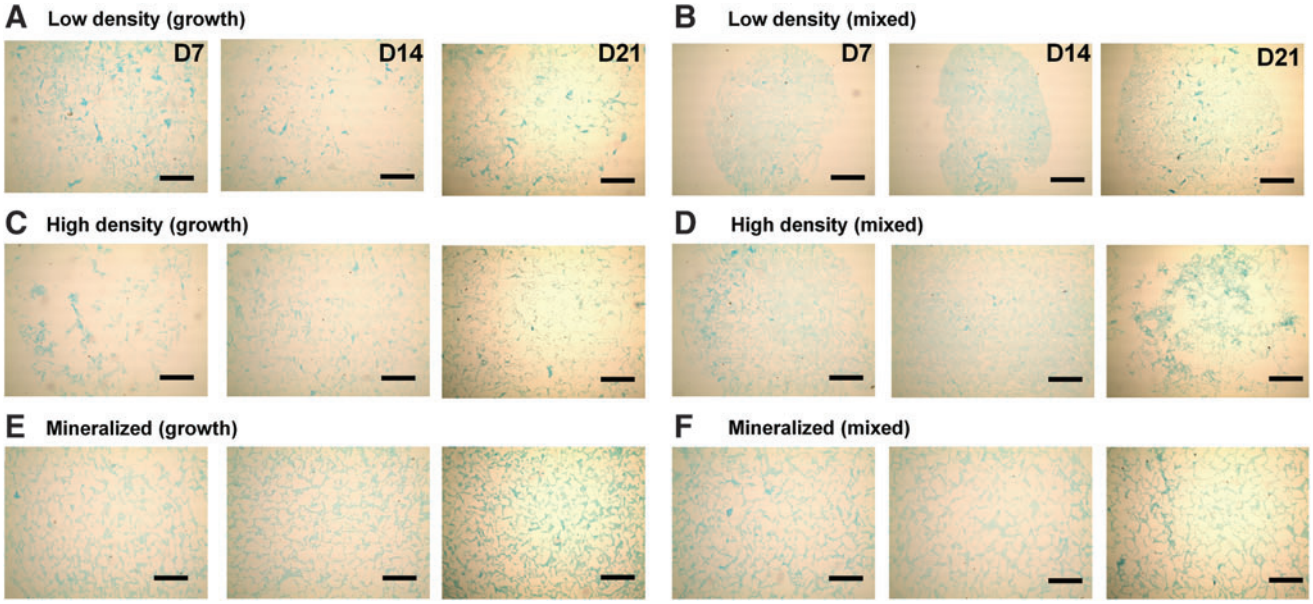

FIG. 6. Alcian blue staining of scaffold sections. Histology sections reveal differential GAG content as a function of scaffold type and media treatment with higher GAG levels initially in the lower density mixed groups, but higher levels in the high-density mixed group by day 21. **(A)** Low density (growth), **(B)** low density (mixed), **(C)** high density (growth), **(D)** high density (mixed), **(E)** mineralized (growth), **(F)** mineralized (mixed). Scale bars: 500 μm. Color images available online at www.liebertpub.com/tea

supplements. Previous work with CG scaffolds and other materials had shown that a lower elastic modulus led to increased contraction, cellular condensation, and chondrogenic response,[17,35–37] while the increased elastic modulus and mineral content promoted a more osteogenic phenotype.[37–39] However, these efforts focused on generating biomaterials for monolithic tissue applications using single media (osteogenic, chondrogenic) formulations. For this study, we hypothesized that the lower density nonmineralized scaffolds would promote more of a chondrogenic phenotype mediated by contraction-induced cellular condensation, while the mineralized scaffolds would facilitate osteogenesis in the presence of joint chondrogenic–osteogenic signals.

We first tracked the MSC metabolic activity and scaffold contraction over the course of a 3-week *in vitro* culture period (Fig. 1). Cells were metabolically active in all scaffold types, although there was a dip in the metabolic activity in the low-density nonmineralized group from day 7 to 14, consistent with previous results in contracting scaffolds.[18,34] There are several possible explanations for this observation, including cell death due to reduced permeability following cell-mediated contraction as well as differentiation to a less metabolically active cell type (e.g., MSC to chondrocyte or osteoblast). To further investigate our hypotheses about the influence of a scaffold's physical properties in the presence of competing signals, we next examined the expression of a selection of osteogenic and chondrogenic markers.

We assessed the expression of chondrogenic genes *COL2A1*, *ACAN*, and *SOX9* as well as osteogenic genes *RUNX2*, *BSP*, *ALP*, and *OCN* over 3 weeks of culture. Not surprisingly, the expression levels of all three chondrogenic markers were depressed for the mineralized scaffolds at day 21 (Fig. 2). Interestingly, the higher density nonmineralized scaffolds surpassed the low-density nonmineralized scaffolds in expression of *COL2A1* and *ACAN* by day 21, despite reduced scaffold contractions. These results differ markedly from previously observed trends with these scaffolds when cultured in pure chondrogenic differentiation media, where CG scaffolds with a lower relative or crosslinking density supported increased cellular condensation and chondrogenesis[35,37] (Supplementary Fig. S1A; Supplementary Data are available online at www.liebertpub.com/tea). This shows that in the presence of multiple differentiation signals, scaffold contraction and cellular condensation may not be beneficial for driving chondrogenesis. Likewise, in the presence of mixed media supplements, the mineralized scaffold did not appear to drive the most substantial osteogenic response despite previous reports showing that mineralized CG scaffolds in combination with pure osteogenic media promote optimal osteogenesis as measured by mineral content and gene expression[37,38] (Supplementary Fig. S1B). In fact, the low-density scaffold group displayed significantly higher expression of the osteogenic markers *BSP*, *ALP*, and *OCN* at day 21 compared with the other two experimental groups (Fig. 3). These results suggest that a scaffold identified to improve chondrogenesis in chondrogenic media may be best suited for osteogenesis in mixed osteogenic–chondrogenic media conditions. Notably, these results also suggest that separate optimization may be necessary to identify media cocktails to support divergent chondrogenesis and osteogenesis in close spatial order.

To more closely examine the spatial and temporal variations in cellular organization and ECM synthesis within these scaffolds, we performed histological analyses. We looked at H&E (Fig. 4), Alizarin red (Fig. 5), and Alcian blue (Fig. 6) staining to assess cellular infiltration/organization, mineral

production, and GAG synthesis, respectively. In this study, we compared each scaffold type in growth and mixed media to better visualize the influence of media supplementation on the responses we observed. Whereas we did not examine the corresponding gene expression profiles in growth media for this study, previous work with these scaffolds has shown minor differences in MSC transcriptomic profiles when cultured in nonsupplemented growth media.[16,37,39] Histological results typically correlated well with the observed gene expression profiles. H&E staining clearly revealed increased contraction and cellular condensation in the low-density mixed media group (Fig. 4). Whereas there was little mineral deposition in the nonmineralized scaffold groups at days 7 or 14, by day 21, Alizarin red staining revealed robust mineralization in the low-density mixed media group compared with the growth media control (Fig. 5), corroborating the osteogenic gene expression results. Similarly, although Alcian blue staining was initially stronger in the lower density groups, by day 21, the strongest staining appeared to be in the high-density, mixed media group (Fig. 6), which mirrored the results of the chondrogenic gene expression analyses.

The discrepancy between previously reported single media results and these mixed media results was initially confounding. However, the kinetics of MSC-mediated scaffold contraction may offer a compelling case to resolve these findings. One possible explanation for the phenotypic switch in the lower density nonmineralized scaffolds between day 14 (higher GAG content) and day 21 (robust mineralization, upregulation of osteogenic genes) is the occurrence of endochondral ossification. Keogh *et al.* previously observed accelerated osteogenic maturation of MC3T3-seeded CG scaffolds with lower crosslinking density (increased contraction).[40] Our noted differences in contraction may suggest that a similar mechanism could be driving the response observed here.

Another possible driver of osteogenesis in the low-density scaffold group could be local stiffening of the extracellular environment following contraction. We explored this possibility using the cellular solids theory to predict changes in the elastic modulus for contracted versus noncontracted scaffolds. Considering that the low density nonmineralized scaffold contracted to about half of its original length in each dimension, this represents a reduction in volume by about a factor of 8 and, therefore, an increase in relative density by the same factor. Cellular solids modeling predicts that the elastic modulus is proportional to the square of relative density,[28] so the significant contraction observed in lower density nonmineralized scaffolds could result in an increase of elastic modulus by a factor of $\sim$60. This indicates that although the low-density nonmineralized scaffolds were initially $\sim$20-fold softer than the mineralized scaffolds,[41,42] contraction-induced remodeling could result in the low-density nonmineralized scaffold being $\sim$3-fold stiffer than the mineralized scaffold variant.

The results of this study suggest a disconnect between conventional single media strategies for driving stem cell-lineage specification *in vitro* and the multimodal approaches needed for multitissue interface engineering, where many signals work in concert *in vivo*. Notably, results from *in vitro* mixed media supplementation suggested unexpected roles of scaffold relative density and mineralization in biasing MSC differentiation toward fibrocartilage and bone. Importantly, these results suggest that nonobvious modifications to biomaterial biophysical properties and soluble factor supplementation may be necessary to selectively enhance or repress disparate differentiation events. Given that we and others have recently begun to demonstrate approaches to generate biomaterials containing spatially graded biophysical properties,[43–46] future studies developing combined biomaterial-growth factor approaches will be critical for repairing complex orthopedic interfaces.

Conclusions

Biomaterials for complex tissue engineering applications must be able to instruct cell behavior in the presence of the multivariate environments encountered *in vivo*. Using a series of CG scaffolds with physical properties optimized to specific components of orthopedic interfaces, we investigated the impact of scaffold relative density and mineral content on MSC-lineage specification in the presence of mixed osteogenic and chondrogenic signals. We found that mineralized scaffolds were able to suppress chondrogenic outcomes compared with the two nonmineralized variants investigated as evidenced by gene expression and histological analyses. Whereas the higher density nonmineralized scaffold elicited a greater chondrogenic response than the mineralized scaffold, the more surprising result was the heightened osteogenic response observed in the lower density, nonmineralized scaffold group with heightened chondrogenesis occurring in the higher density, nonmineralized group. This unexpected response may be due to local stiffening of the extracellular environment due to cell-mediated scaffold contraction. The increased cell density as a result of contraction may have also accelerated the kinetics of MSC differentiation and maturation, leading to a response similar to endochondral ossification. These results will inform ongoing work in our laboratory designing multicompartment scaffolds for graded tissue regeneration.

Acknowledgments

The authors would like to acknowledge Donna Epps (IGB, UIUC) for assistance with histology, Daniel Weisgerber (MSE, UIUC) for preparation of mineral scaffolds, and the IGB Core Facilities for assistance with real-time PCR. The authors are grateful for the funding for this study provided by the Chemistry-Biology Interface Training Program NIH T32GM070421 (S.R.C.), NSF 1105300 (B.A.H.), the Chemical and Biomolecular Engineering Dept. (B.A.H.), and the Institute for Genomic Biology (B.A.H.) at the University of Illinois at Urbana-Champaign.

Disclosure Statement

No competing financial interests exist.

References

1. Galatz, L., Rothermich, S., VanderPloeg, K., Petersen, B., Sandell, L., and Thomopoulos, S. Development of the supraspinatus tendon-to-bone insertion: localized expression of extracellular matrix and growth factor genes. J Orthop Res **25,** 1621, 2007.
2. Galatz, L.M., Sandell, L.J., Rothermich, S.Y., Das, R., Mastny, A., Havlioglu, N., *et al.* Characteristics of the rat

supraspinatus tendon during tendon-to-bone healing after acute injury. J Orthop Res **24,** 541, 2006.
3. Genin, G.M., Kent, A., Birman, V., Wopenka, B., Pasteris, J.D., Marquez, P.J., *et al.* Functional grading of mineral and collagen in the attachment of tendon to bone. Biophys J **97,** 976, 2009.
4. Kuo, C.K., Petersen, B.C., and Tuan, R.S. Spatiotemporal protein distribution of TGF-betas, their receptors, and extracellular matrix molecules during embryonic tendon development. Dev Dyn **237,** 1477, 2008.
5. Fox, A.J.S., Bedi, A., Deng, X.H., Ying, H., Harris, P.E., Warren, R.F., *et al.* Diabetes mellitus alters the mechanical properties of the native tendon in an experimental rat model. J Orthopaed Res **29,** 880, 2011.
6. Xu, Y.H., and Murrell, G.A.C. The basic science of tendinopathy. Clin Orthop Relat Res **466,** 1528, 2008.
7. Ker, E.D., Chu, B., Phillippi, J.A., Gharaibeh, B., Huard, J., Weiss, L.E., *et al.* Engineering spatial control of multiple differentiation fates within a stem cell population. Biomaterials **32,** 3413, 2011.
8. Pittenger, M.F., Mackay, A.M., Beck, S.C., Jaiswal, R.K., Douglas, R., Mosca, J.D., *et al.* Multilineage potential of adult human mesenchymal stem cells. Science **284,** 143, 1999.
9. Kilian, K.A., Bugarija, B., Lahn, B.T., and Mrksich, M. Geometric cues for directing the differentiation of mesenchymal stem cells. Proc Natl Acad Sci U S A **107,** 4872, 2010.
10. Khetan, S., and Burdick, J.A. Patterning network structure to spatially control cellular remodeling and stem cell fate within 3-dimensional hydrogels. Biomaterials **31,** 8228, 2010.
11. Wagner, D.R., Lindsey, D.P., Li, K.W., Tummala, P., Chandran, S.E., Smith, R.L., *et al.* Hydrostatic pressure enhances chondrogenic differentiation of human bone marrow stromal cells in osteochondrogenic medium. Ann Biomed Eng **36,** 813, 2008.
12. Yannas, I.V., Lee, E., Orgill, D.P., Skrabut, E.M., and Murphy, G.F. Synthesis and characterization of a model extracellular matrix that induces partial regeneration of adult mammalian skin. Proc Natl Acad Sci U S A **86,** 933, 1989.
13. Chamberlain, L.J., Yannas, I.V., Hsu, H.P., Strichartz, G., and Spector, M. Collagen-GAG substrate enhances the quality of nerve regeneration through collagen tubes up to level of autograft. Exp Neurol **154,** 315, 1998.
14. O'Brien, F.J., Harley, B.A., Yannas, I.V., and Gibson, L.J. The effect of pore size on cell adhesion in collagen-GAG scaffolds. Biomaterials **26,** 433, 2005.
15. Harley, B.A.C., Kim, H.D., Zaman, M.H., Yannas, I.V., Lauffenburger, D.A., and Gibson, L.J. Microarchitecture of three-dimensional scaffolds influences cell migration behavior via junction interactions. Biophys J **95,** 4013, 2008.
16. Farrell, E., O'Brien, F.J., Doyle, P., Fischer, J., Yannas, I., Harley, B.A., *et al.* A collagen-glycosaminoglycan scaffold supports adult rat mesenchymal stem cell differentiation along osteogenic and chondrogenic routes. Tissue Eng **12,** 459, 2006.
17. Vickers, S.M., Squitieri, L.S., and Spector, M. Effects of cross-linking type II collagen-GAG scaffolds on chondrogenesis *in vitro*: dynamic pore reduction promotes cartilage formation. Tissue Eng **12,** 1345, 2006.
18. Caliari, S.R., Weisgerber, D.W., Ramirez, M.A., Kelkhoff, D.O., and Harley, B.A.C. The influence of collagen-glycosaminoglycan scaffold relative density and microstructural anisotropy on tenocyte bioactivity and transcriptomic stability. J Mech Behav Biomed Mater **11,** 27, 2012.
19. Harley, B.A., Lynn, A.K., Wissner-Gross, Z., Bonfield, W., Yannas, I.V., and Gibson, L.J. Design of a multiphase osteochondral scaffold. II. Fabrication of a mineralized collagen-glycosaminoglycan scaffold. J Biomed Mater Res A **92,** 1066, 2010.
20. Yannas, I.V., Burke, J.F., Gordon, P.L., Huang, C., and Rubenstein, R.H. Design of an artificial skin. II. Control of chemical composition. J Biomed Mater Res **14,** 107, 1980.
21. Lynn, A.K., Best, S.M., Cameron, R.E., Harley, B.A., Yannas, I.V., Gibson, L.J., *et al.* Design of a multiphase osteochondral scaffold. I. Control of chemical composition. J Biomed Mater Res A **92,** 1057, 2010.
22. O'Brien, F.J., Harley, B.A., Yannas, I.V., and Gibson, L. Influence of freezing rate on pore structure in freeze-dried collagen-GAG scaffolds. Biomaterials **25,** 1077, 2004.
23. Weisgerber, D.W., Kelkhoff, D.O., Caliari, S.R., and Harley, B.A.C. The impact of discrete compartments of a multi-compartment collagen-GAG scaffold on overall construct biophysical properties. J Mech Behav Biomed Mater **28,** 26, 2013.
24. Olde Damink, L.H., Dijkstra, P.J., van Luyn, M.J., van Wachem, P.B., Nieuwenhuis, P., and Feijen, J. Cross-linking of dermal sheep collagen using a water-soluble carbodiimide. Biomaterials **17,** 765, 1996.
25. Harley, B.A., Leung, J.H., Silva, E.C., and Gibson, L.J. Mechanical characterization of collagen-glycosaminoglycan scaffolds. Acta Biomater **3,** 463, 2007.
26. Tierney, C.M., Jaasma, M.J., and O'Brien, F.J. Osteoblast activity on collagen-GAG scaffolds is affected by collagen and GAG concentrations. J Biomed Mater Res A **91,** 92, 2009.
27. Spilker, M.H., Asano, K., Yannas, I.V., and Spector, M. Contraction of collagen-glycosaminoglycan matrices by peripheral nerve cells *in vitro*. Biomaterials **22,** 1085, 2001.
28. Gibson, L.J., Ashby, M.F., and Harley, B.A. Cellular Materials in Nature and Medicine. Cambridge, United Kingdom: Cambridge University Press, 2010.
29. Duffy, G.P., McFadden, T.M., Byrne, E.M., Gill, S.L., Farrell, E., and O'Brien, F.J. Towards *in vitro* vascularisation of collagen-GAG scaffolds. Eur Cell Mater **21,** 15, 2011.
30. Frank, O., Heim, M., Jakob, M., Barbero, A., Schafer, D., Bendik, I., *et al.* Real-time quantitative RT-PCR analysis of human bone marrow stromal cells during osteogenic differentiation *in vitro*. J Cell Biochem **85,** 737, 2002.
31. Zhou, J., Xu, C., Wu, G., Cao, X., Zhang, L., Zhai, Z., *et al.* *In vitro* generation of osteochondral differentiation of human marrow mesenchymal stem cells in novel collagen-hydroxyapatite layered scaffolds. Acta Biomater **7,** 3999, 2011.
32. Pek, Y.S., Spector, M., Yannas, I.V., and Gibson, L.J. Degradation of a collagen-chondroitin-6-sulfate matrix by collagenase and by chondroitinase. Biomaterials **25,** 473, 2004.
33. Freyman, T.M., Yannas, I.V., Pek, Y.-S., Yokoo, R., and Gibson, L.J. Micromechanics of fibroblast contraction of a collagen-GAG matrix. Exp Cell Res **269,** 140, 2001.
34. Torres, D.S., Freyman, T.M., Yannas, I.V., and Spector, M. Tendon cell contraction of collagen-GAG matrices *in vitro*: effect of cross-linking. Biomaterials **21,** 1607, 2000.
35. Vickers, S.M., Gotterbarm, T., and Spector, M. Cross-linking affects cellular condensation and chondrogenesis in type II

collagen-GAG scaffolds seeded with bone marrow-derived mesenchymal stem cells. J Orthop Res **28,** 1184, 2010.
36. Tang, S.Q., and Spector, M. Incorporation of hyaluronic acid into collagen scaffolds for the control of chondrocyte-mediated contraction and chondrogenesis. Biomed Mater **2,** S135, 2007.
37. Caliari, S.R., and Harley, B.A.C. Structural and biochemical modification of a collagen scaffold to selectively enhance MSC tenogenic, chondrogenic, and osteogenic differentiation. Adv Healthc Mater 2014 [Epub ahead of print]; DOI: 10.1002/adhm.201300646.
38. Curtin, C.M., Cunniffe, G.M., Lyons, F.G., Bessho, K., Dickson, G.R., Duffy, G.P., *et al.* Innovative collagen nano-hydroxyapatite scaffolds offer a highly efficient non-viral gene delivery platform for stem cell-mediated bone formation. Adv Mater **24,** 749, 2012.
39. Murphy, C.M., Matsiko, A., Haugh, M.G., Gleeson, J.P., and O'Brien, F.J. Mesenchymal stem cell fate is regulated by the composition and mechanical properties of collagen-glycosaminoglycan scaffolds. J Mech Behav Biomed Mater **11,** 53, 2012.
40. Keogh, M.B., O'Brien, F.J., and Daly, J.S. Substrate stiffness and contractile behaviour modulate the functional maturation of osteoblasts on a collagen-GAG scaffold. Acta Biomater **6,** 4305, 2010.
41. Kanungo, B.P., and Gibson, L.J. Density-property relationships in collagen-glycosaminoglycan scaffolds. Acta Biomater **6,** 344, 2010.
42. Kanungo, B.P., and Gibson, L.J. Density-property relationships in mineralized collagen-glycosaminoglycan scaffolds. Acta Biomater **5,** 1006, 2009.
43. Harley, B.A., Lynn, A.K., Wissner-Gross, Z., Bonfield, W., Yannas, I.V., and Gibson, L.J. Design of a multiphase osteochondral scaffold III: fabrication of layered scaffolds with continuous interfaces. J Biomed Mater Res A **92,** 1078, 2010.
44. Erisken, C., Kalyon, D.M., and Wang, H.J. Functionally graded electrospun polycaprolactone and beta-tricalcium phosphate nanocomposites for tissue engineering applications. Biomaterials **29,** 4065, 2008.
45. Xie, J., Li, X., Lipner, J., Manning, C.N., Schwartz, A.G., Thomopoulos, S., *et al.* ''Aligned-to-random'' nanofiber scaffolds for mimicking the structure of the tendon-to-bone insertion site. Nanoscale **2,** 923, 2010.
46. Li, X., Xie, J., Lipner, J., Yuan, X., Thomopoulos, S., and Xia, Y. Nanofiber scaffolds with gradations in mineral content for mimicking the tendon-to-bone insertion site. Nano Lett **9,** 2763, 2009.

Address correspondence to:
Brendan A.C. Harley, ScD
Department of Chemical and Biomolecular Engineering
University of Illinois at Urbana-Champaign
110 Roger Adams Laboratory
600 S. Mathews Avenue
Urbana, IL 61801

E-mail: bharley@illinois.edu

Received: July 2, 2013
Accepted: February 24, 2014
Online Publication Date: March 24, 2014